A New Photodiode Readout Scheme for High Resolution Scintillation Crystal Arrays

Craig S. Levin and Edward J. Hoffman

Division of Nuclear Medicine and Biophysics, UCLA School of Medicine
Los Angeles CA 90095-6948

Abstract

We are exploring the possibility of using PIN photodiodes to readout the scintillation crystals used in Positron Emission Tomography (PET) detector designs. Solid state photodetectors typically have a lower signal to noise ratio than photomultiplier tubes (PMTs). However, they have the advantage of compactness, and, thus, scintillation crystal readout schemes not available to PMTs because of their size and geometry limitations, are readily available to photodiodes. With current PET detector designs, only a small fraction of the available scintillation light created from 511 keV gamma ray interactions within the crystal is collected. Scintillation light collection studies were performed for several crystal geometries and surface treatments using both simulations and measurements. In this report, we present a feasible photodiode readout scheme that allows greater than 90% of the available scintillation light created in either BGO or LSO scintillation crystals to be collected by the photodetector. This improvement in light collection with the photodiode readout somewhat compensates for its lower inherent signal to noise ratios and makes it feasible for use in PET. In addition, a coincident timing spectrum resolution of 3.5 ns FWHM was measured using small crystals of LSO, one coupled to a photodiode, the other to a PMT.

I. INTRODUCTION

In current Nuclear Medicine scintillation camera instrumentation, photomultiplier tubes (PMT) are used for scintillation light readout. These devices have the advantages of high gain and signal-noise-ratios (SNR). However, disadvantages of the PMT are the bulkiness and the cost. In most Positron Emission Tomography (PET) detector designs described in the literature, arrays of long and narrow discrete or pseudo-discrete BGO or LSO scintillation crystals are coupled either one to one to PMTs [1-3] or to four PMTs [4-6], respectively. Various reflectors and surface treatments are used to channel the light towards the small end faces of the crystals where the light is readout. The fraction of the available scintillation light collected from a 511 keV interaction within a given crystal generally decreases as the ratio of the crystal length to cross-sectional area increases. This dependence is due to the increased number of reflections scintillation photons encounter within longer and narrower crystals. In addition, if the side faces of these long and thin crystals are not highly polished, there is less chance that a scintillation photon will undergo total internal reflection, further diminishing the light yield. The result is that in current PET detector designs, only a small fraction of the scintillation light available from 511 keV interactions within the crystal is collected. Ideally, it would be best to readout long and narrow scintillation crystals from all sides or at least from the largest side faces. However, for compact scintillation crystal arrays, this ideal readout is impossible with PMTs, because of their size and geometry, and only crystal end readout is possible.

Solid state photodetectors, such as silicon PIN photodiodes (PDs) have the advantage of compactness. Scintillation crystal readout schemes not available to PMTs because of their bulkiness, are readily available to PDs. For example, the side faces of long and narrow crystals in an array can be readout using PDs, provided the PDs are thin enough to insert in between crystal planes without an unusual increase in dead area. PDs have other advantages over PMTs such as higher quantum efficiency and lower cost. However, as devices, PDs have a lower SNR than photomultiplier tubes (PMTs) due to capacitive noise and dark current. Others [7-17] have proposed using arrays of PDs and avalanche photodiodes (APDs) to readout crystal arrays in PET. Scintillation light collection studies were performed for several crystal geometries and surface treatments using both simulations and measurements. In this report, we present a feasible scintillation crystal room temperature photodiode readout scheme that allows greater than 90% of the available scintillation light created in either BGO or LSO to be collected by the photodetector. This improvement in light collection with the photodiode readout somewhat compensates for its lower inherent SNR and makes it feasible for use in PET. We demonstrate that the proposed scheme has sufficient SNR required for PET.

II. METHODS

A. Potential Photodiode Readout Scheme

Figure 1 depicts a potential photodiode readout scheme for scintillation crystal arrays used in PET. Readout of the side face of a long and narrow crystal has the advantage of collecting a larger fraction of the scintillation light created in a crystal by a 511 keV gamma ray interaction compared to the standard end face readout. The amount of light collected from long and narrow crystals depends highly on the number of interactions the optical photons have with the crystal surfaces before collection. This number of interactions varies as the length of the crystal divided by the cross-sectional area. Because of this fact, for long, narrow crystals used in PET detector arrays, the optimal readout (least reflections before readout) would be from the sides rather than small ends of the crystals. Thin (<250μm) 1-D arrays of room temperature PD strips could accomplish this side readout. These PD arrays could easily fit in between crystal planes without introducing any more dead area than that already present in current designs which have ~250-400μm of white reflector material between crystals. The PD cannot be made with too thin a depletion region since this would imply large terminal capacitance and, therefore, higher noise. This type of readout scheme would be unavailable to multi-channel PMT designs. The photodiodes would be readout with an ASIC array of miniature low noise charge sensitive preamplifiers built directly under the array.

0-7803-3534-1/97 10.00©1997IEEE

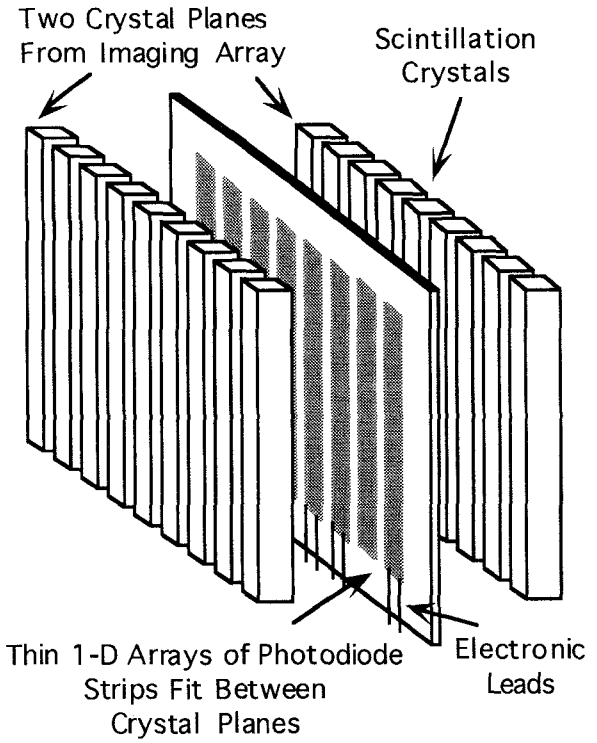

Figure 1. Schematic of a potential photodiode readout of a scintillation crystal array (only two crystal planes shown). The thickness of 1-D array of photodiode strips can be made < 250μm to minimize the dead area between crystal planes.

B. Monte Carlo Simulations

Optical photon tracking Monte Carlo simulations were performed with DETECT [18] to determine light output characteristics of BGO and LSO scintillation crystals for various readout conditions. We assume that a gamma ray interaction will create a point source of light. A 2x2 mm^3 (high resolution) cross-sectional crystal area was used for these studies. We use a diffuse, 98% reflective surface on the crystal faces not connected to the photodetector. Since we are interested only in relative light collection values, we assumed a photodetector quantum efficiency of 100%. The average fraction of available scintillation light collected for side vs. end face readout of a scintillation crystal was determined as a function of its length. We determine this average by weighting the calculated fraction of collected light for a given interaction point within a crystal with the gamma ray interaction probability of that location. The 511 keV absorption lengths used for LSO and BGO are 11.3 and 10.6 mm, respectively. The study was performed for both ground as well as polished crystal faces. We do this because in practice it is not always possible to have highly polished crystal faces. Ground side faces will further diminish the fraction of the available scintillation light collected when using readout of the end face of a crystal. This decrease will be magnified for longer and narrower crystals.

C. Experimental Measurements

To demonstrate that the PD readout scheme has sufficient SNR for PET, energy spectra measurements were performed with both a PD and a PMT, for comparison. The PD was a Hamamatsu S3588 (3 x 30 mm^2 active area). Typical dark current specifications of this PD range from 3-10 nA at room temperature . The PD was biased with -70 V and readout with an ORTEC 142A charge sensitive preamplifier and amplified and shaped with a CANBERRA 2021 (shaping time: 250 ns and 1 μs for LSO and BGO, respectively). A ^{22}Na (511 keV) gamma ray source was used for the measurements. Two sizes of LSO crystals (2x2x10mm^3 and 2.5x2.5x20mm^3, both highly polished on all sides) and four sizes of BGO crystals (1.5x1.5x10mm^3, sides and one end ground, the other end "pseudo-polished", 2x2x10mm^3, sides and ends polished, 2x2x20mm^3, sides and ends "pseudo-polished", and 2x2x30mm^3, sides and ends "pseudo-polished") were used, each coupled via optical grease to the PD. The sides of the crystals not in contact with the PD were wrapped in white Teflon as a reflector. Measured results were compared to those obtained by simulations.

Coincidence timing spectra were measured using the 2.5x2.5x20mm^3 LSO crystal coupled to the PD and a 4x4x10mm^3 LSO crystal coupled to an RCA C31024 PMT. Preamplification for the PMT was achieved with the ORTEC 9301. Both the PD and PMT channels were filtered with the ORTEC 579 Timing Filter Amplifier and the timing was picked off with an ORTEC 935 Quad Constant Fraction Discriminator (CFD). The CFD threshold was set above the noise level in both channels. The PMT channel served as a start for the TENELEC TC863 Time to Amplitude Converter (TAC) and the PD channel provided the stop. A delay (ORTEC 425) positioned the timing spectra on the digitized TAC value axis.

III. RESULTS

A. Simulations

Table 1 summarizes the results from the Monte Carlo simulations of light collected. We assumed that a gamma ray interaction creates a point source of scintillation light within a crystal. Light collected in 2x2x10 mm^3, 2x2x20 mm^3, and 2x2x30 mm^3 crystals was studied with both end face (2x2 mm^2 area) and side face (2x10 mm^2 area, 2x20 mm^2 area, and 2x30 mm^2 area) readout of the scintillation light. For each case, both perfectly polished and highly ground surface treatment results are shown. In reality, it may only be possible to achieve somewhere between these idealized surface treatments. The values in the table are the average fraction (%) of the total available light collected. The average was calculated over several origins of the source of light (depths of interaction) within a crystal by weighting the location of the origin with the interaction probability at that location.

Table 1. Comparison of light collected for side and end readout schemes for 3 sizes and 2 surface treatments of LSO and BGO crystals. Values shown are % of available light collected.

Readout/ Surfaces	2x2x10 mm^3 LSO	2x2x10 mm^3 BGO	2x2x20 mm^3 LSO	2x2x20 mm^3 BGO	2x2x30 mm^3 LSO	2x2x30 mm^3 BGO
End/ Polished	61.9	63.8	55.3	53.1	50.0	44.6
Side/ Polished	89.9	87.1	90.6	88.9	91.4	88.3
End/ Ground	58.5	49.8	37.7	31.1	23.9	19.1
Side/ Ground	86.7	83.2	88.3	83.0	89.0	83.3

In Table 1, we see that the light collection fraction is relatively insensitive to crystal length and surface treatment when readout from the side. In addition, for a series of simulations performed with narrower (< 2mm wide) crystals and side readout, we saw the light collected was fairly independent of crystal width. Thus, side readout opens the possibility of reducing the width of the crystals below 2 mm (and, thus, improving intrinsic resolution) while still collecting a high fraction of the available scintillation light. Using end readout, however, the predicted light collection strongly depends on the crystal length, width and surfaces.

From the table we also see the clear improvement in the amount of scintillation light collected for side compared to end readout. The improvement is huge when the crystal is ground ("lossy") and significant even when the crystal surface is perfectly specular. The improvement is also greater for longer crystals, due to the larger number of reflections photons undergo before exiting a crystal end compared to side face. For perfectly polished crystals (the ideal case), the predicted improvement of side over end readout of the scintillation light is roughly 45, 64 and 83% for the 2x2x10mm^3 , 2x2x20mm^3, 2x2x30mm^3 size LSO crystals, respectively, and 37, 67 and 98 % for the 2x2x10mm^3, 2x2x20mm^3, 2x2x30mm^3 size BGO crystals, respectively. For narrower crystal widths simulated, these differences were larger.

The large advantage of side over end readout becomes most evident for less polished crystals. For 2x2x10mm^3, 2x2x20mm^3, and the 2x2x30mm^3 size ground crystals, the predicted improvement in light collected for side over end readout is, respectively, 48, 120 and 272% for LSO, and 67, 167, and 336% for BGO. These results are important since in reality it is not easy to obtain a large quantity of perfectly polished crystals and the difference in light collected between the two surface treatments is not significant for side readout of the scintillation light. For all crystal lengths and widths studied, with side readout, the fraction of available light collected was greater than 88% (83%) for highly polished (ground) crystal surfaces. In practice, this side readout scheme of a scintillation crystal array can only be realized with the compactness of a thin solid state detector.

B. Measurements

To demonstrate that the PD readout scheme proposed has sufficient SNR for PET, the important comparison to make is between energy measurements performed with scintillation crystals readout from the side face with a PD and from the end face with a PMT. Figure 2 shows this comparison for the 2x2x10mm^3 and 2.5x2.5x20mm^3 sizes of LSO crystals (large graphs), and for the 1.5x1.5x10mm^3, 2x2x10mm^3, 2x2x20mm^3, and 2x2x30mm^3 sizes of BGO (small graphs). The spectroscopy amplifier gain used for the PMT data was approximately twice that used for the PD. To facilitate comparisons, all PD spectra presented have the same gain and ADC channel scale on the plots. The same is true for all PMT spectra. The measured energy resolution of the 511 keV photopeak from ^{22}Na was 24% FWHM for both the PD side and PMT end readout using the 2x2x10mm^3 LSO crystal. For the 2.5x2.5x20mm^3 LSO crystal, the corresponding values were 23% for the PD and 21% for the PMT. For the LSO measurements, even though the PMT gain is higher and the dark current is lower than for the PD, with PMT end face readout of the crystal, there is no

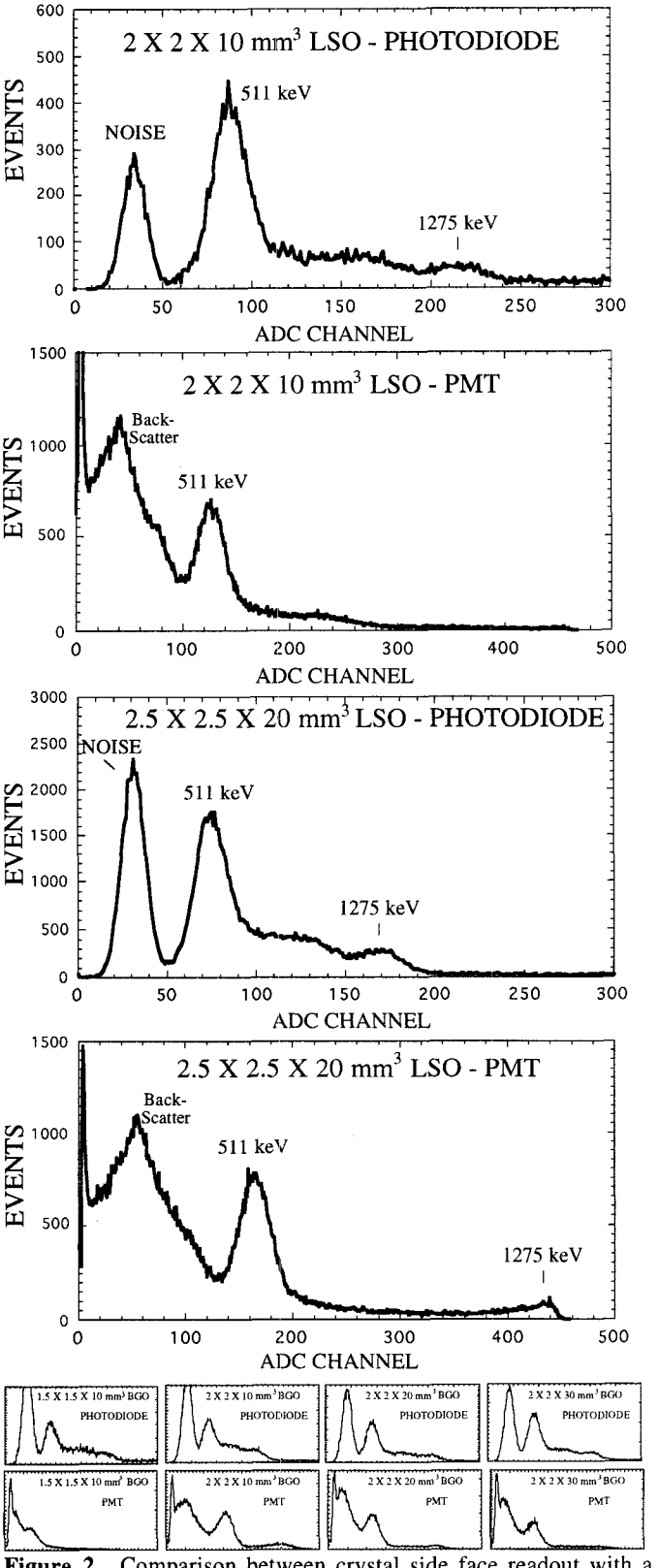

Figure 2. Comparison between crystal side face readout with a photodiode and end face readout with a PMT, for long and narrow LSO (top large plots) and BGO (bottom small plots) crystals (sizes shown on graphs) ^{22}Na was used for the measurements.. Scintillation photons undergo, on average, more surface reflections when readout through the end vs. the side of the crystal. Thus, for the PMT spectra, the pulse height and energy resolution degrade as crystal length increases, the width decreases and for less polished surfaces. For the PD side readout spectra, light collection properties are relatively insensitive to these crystal parameters. See text for energy resolution values.

significant signal to noise gain over the PD side face readout. This is the case since only a small fraction of the available scintillation light is collected with end readout. In addition, as predicted by the simulations, the PD results for pulse height (photopeak position) and energy resolution are insensitive to the length and width of the crystal. However, because of the higher noise shoulder of the PD, the lower energy scatter continuum is not resolved ("in the noise").

The BGO spectra plotted on a smaller scale on the bottom of Figure 2 show the PD measured results on top and that for the PMT underneath for easy comparison. The corresponding crystal sizes are, from left to right, $1.5x1.5x10mm^3$, $2x2x10mm^3$, $2x2x20mm^3$, and $2x2x30mm^3$, and the respective energy resolutions at 511 keV are 33, 30, 33, and 30 % FWHM for the side PD readout and 70, 35, 42, and 45 % for the BGO end readout. In all BGO cases, the energy resolution is superior for the PD side readout combination. This fact is especially seen for the 1.5 mm wide ground crystals, where one can barely resolve the photopeak measured with a PMT from the end. On the other hand, as predicted from the simulations, the pulse height and energy resolution are fairly insensitive to both crystal length, width and surface treatment for side readout.

Because we have the $2x2x10mm^3$, $2x2x20mm^3$, and $2x2x30mm^3$ crystal sizes of BGO, we can directly compare simulation results of Table 1 with measurements. Figure 3 (top) shows two ^{22}Na spectra measured with the 20 and 30 mm long BGO crystals for side and end readout with a PMT. There is a clear improvement in light collection with side readout as seen by the higher photopeak position. For the 10, 20, and 30 mm lengths this improvement was measured to be 23, 26 and 65 %, respectively (bottom). The corresponding improvement predicted from simulation of polished BGO crystals was 36, 41, and 98%, respectively. The relatively large discrepancy between simulated and measured values might be explained by (1) In the simulations, the crystal face in contact with the photodetector was always assumed to be polished. In the measurements, the crystal was pseudo-

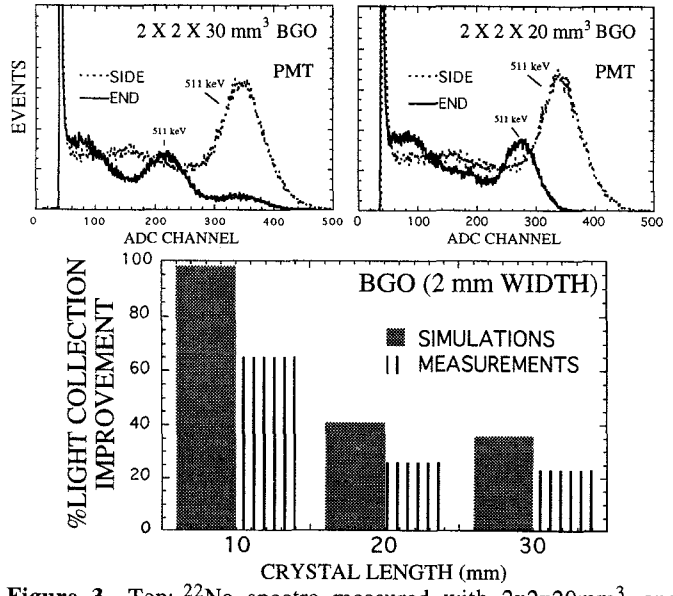

Figure 3. Top: ^{22}Na spectra measured with $2x2x20mm^3$, and $2x2x30mm^3$ BGO and PMT for side and end readout. See Figure legends. Below: Comparison between simulations and measurements of light collection improvement of side over end readout.

polished/semi-ground at best; (2) The calculation of the average light collection fraction from the simulation may have been weighted incorrectly with different points of light production (depth of interaction). However, the important point is that both simulations and measurements show side readout provides a large improvement in light collection efficiency over end readout, especially for longer and narrower crystals.

A crucial requirement for a PD readout for PET is that excellent coincident timing for annihilation gamma rays is possible. Figure 4 demonstrates that this condition is satisfied using ^{22}Na source irradiation and side readout. A coincidence timing resolution of 3.5 ns FWHM was measured with the LSO/PMT combination as the TAC Start and the LSO/PD as a Stop. Even though the CFD threshold was set above the PD noise shoulder, noise still contaminates the measured results as seen by the tail on the slow end of the timing spectrum (right side). Because of this tail, the measured FWTM resolution is 8.3 ns. Fitting a gaussian to the faster (left side) of the peak, we obtain a resolution of 680 ns FWHM, which one may roughly interpret as the timing resolution possible with LSO/PMT in both start and stop channels. This compares fairly well to previous results reported for LSO/PMT [19].

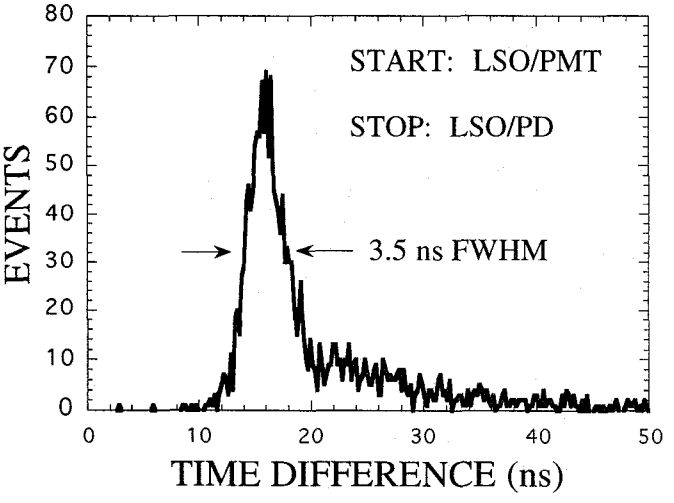

Figure 4. Measured coincident timing spectrum. Start: $4x4x10mm^3$ LSO crystal on a PMT. Stop: $2.5x2.5x20mm^3$ LSO crystal on a photodiode. A coincidence timing resolution of 3.5 ns FWHM was measured indicating good timing capability for PET with a photodiode readout.

IV. SUMMARY

We have proposed a feasible solid state readout scheme for PET scintillation crystal arrays involving strips of silicon PIN photodiodes (PD) in between crystal planes. The strips readout the crystals from the large side faces of long and narrow crystals as opposed to the ends. Because the photodetector planes are very thin no unusual dead area between crystals is introduced. The PD cannot be too thin because the device capacitance, and, therefore, noise increases with decreasing thickness. We have shown that with the side readout of the light, the fraction of the available scintillation light collected from 511 keV interactions is high (>90% for polished LSO) and roughly independent of the crystal length, width and surface treatments. This implies that extremely narrow crystals can be used, for higher detector resolution , if

desired. In fact, energy resolution will improve as the PD area decreases due to a reduction in dark current and capacitive noise. However, in that case more channels are required to cover the same area. In addition, there is a limit to this resolution: if the thickness of the PD becomes a significant fraction of the crystal width, the dead area fraction of the array increases. Although we described this new readout scheme for use in PET, it can be used for any crystal array application.

With the conventional crystal end readout, the light collected is only a small fraction of that available and is highly dependent on crystal parameters. We have demonstrated comparable and, in some cases, better energy resolution characteristics with scintillation crystals coupled to a PD with side readout than with a PMT and the standard end readout. The boost in signal to noise ratio achieved with the side readout allows the LSO/PD combination to provide excellent coincident timing resolution. In principal, other types of reliable solid state detector devices that can be made thin enough to fit in between planes of scintillation crystal arrays can be used in this readout scheme (APDs, for example).

We note that the PD strips may be coupled one on one to the crystals rather than using a 1-D array of strips as shown in Figure 1. We also note that if depth of gamma ray interaction resolving power is desired for the array, each PD strip could, in principle, be segmented lengthwise. However, this requires more electronic channels for processing. Another possibility is segmenting each crystal in the array into two or more scintillators with different decay time characteristics coupled lengthwise. Pulse shape discrimination could be then used for a depth of interaction measurement, similar in principle to that reported previously [20]. This latter scheme poses no problems as long as the different scintillators used have sufficient light yield to be above the noise shoulder of the PD.

V. ACKNOWLEDGMENTS

This work was supported by grants from the Department of Energy (DE-CO3-87-ER60615), National Institutes of Health (R01-CA56655) and the State of California (IRB-0225).

VI. REFERENCES

[1] Moses, W.W.; Derenzo, S.E.; Geyer, A.B.; Huesman, R.H.; and others. The tuning algorithms used by the Donner 600 crystal tomograph. *IEEE Trans. Nucl. Sci.*, **36**-1:1025-9 (1989).

[2] M. Watanabe, H. Uchida, H. Okada et. al.. A High Resolution PET for Animal Studies. *IEEE Trans. Med. Imag* **11**: 577-80 (1992).

[3] S.R. Cherry, Y. Shao, S. Siegel et al. Optical Fiber Readout of Scintillator Arrays Using a Multi-Channel PMT: A High Resolution PET Detector for Animal Imaging. *IEEE Trans. Nucl. Sci.* **43-3**: 1932-7 (1996).

[4] M.E. Casey and R. Nutt. A Multi-crystal Two Dimensional BGO Detector System for Positron Emission Tomography. *IEEE Trans. Nucl. Sci.* NS-**33**: 460-3 (1986).

[5] M. Dahlbom and E.J. Hoffman. An evaluation of a Two-dimensional Array Detector for High Resolution PET. IEEE Trans. Med. Imag. **7**: 264-72 (1988).

[6] S.R. Cherry, M.P. Tornai, C.S. Levin et al., "A Comparison of PET Detector Modules Employing Rectangular and Round Photomultiplier Tubes. *IEEE Trans Nucl Sci*, NS-42: 1064-8 (1995).

[7] JB Barton, E.J. Hoffman, J.S. Iwanczyk, et. a. A High Resolution Detection System for Positron Emission Tomography. *IEEE Trans Nucl Sci* **NS-30**: 671-5, 1983.

[8] S.E. Derenzo, T.G. Budinger and T. Vuletich. High Resolution Positron Emission Tomography Using Narrow Bismuth Germanate Crystals and Individual Photosensors. *IEEE Trans Nucl Sci* NS-**30**:665-70 (1983).

[9] SE Derenzo. Gamma-ray Spectroscopy Using Small Cooled Bismuth Germanate Scintillators and Silicon Photodiodes. *Nucl Instr Meth* **219**: 117-22 (1984).

[10] M Dahlbom, M.A. Mandelkern, E.J. Hoffman, et. al. Hybrid Mercuric Iodide (HgI_2) -- Gadolinium Orthosilicate (GSO) Detector for PET. IEEE Trans Nucl Sci NS-32: 533-7 (1985).

[11] R. Lecomte, J. Cadorette, A. Jouan, et. al. High Resolution Positron Emission Tomography with a Prototype Camera Based on Solid State Detectors. *IEEE Trans. Nucl. Sci.* NS-37: 805-11 (1990).

[12] W.W. Moses, S.E. Derenzo, et. al. Performance of a PET Detector Module Utilizing an Array of Silicon Photodiodes to Identify the Crystal of Interaction. *IEEE Trans Nucl Sci* **40-4**:1036-40 (1993).

[13] N.H. Clinthorne. Are Hydrogenated Amorphous Silicon Arrays Usable for Tomographic Imaging? *IEEE Nucl Sci Symp and Med Im Conf Rec* **3**: 1692-6 (1993).

[14] C.J. Marriott, J.E. Cadorette, R. Lecomte et. al. High Resolution PET Imaging and Quantitation of Pharmaceutical Biodistributions in a Small Animal Using Avalanche Photodiode Detectors. *J Nucl Med* **35**:1390-7 (1994).

[15] W.W. Moses, S.E. Derenzo, et. al. A Room Temperature LSO/PIN photodiode PET Detector Module That Measures Depth of Interaction. *IEEE Trans Nucl Sci* 42-4:1085-9 (1995).

[16] M.J. Paulus, J.M. Rochelle, D.M. Binkley. Comparison of the Beveled-Edge and Reach-Through APD Structures for PET Applications. *IEEE Nucl Sci Symp and Med Im Conf Rec* **4**: 1864-8 (1994).

[17] C. Schmelz, S.M. Bradbury, I. Holl, E. Lorentz et. al. Feasibility Study of an Avalanche Photodiode Readout for a High Resolution PET with nsec timing resolution. *IEEE Trans Nucl Sci* **42-4**:1080-4 (1995).

[18] G.F. Knoll, T.F. Knoll, T.M. Henderson. Light Collection in Scintillating Detector Composites for Neutron Detection. *IEEE Trans Nucl Sci* **NS**-35-1: 872-5 (1988).

[19] F. Daghighian, P. Shenderov, et. al. Evaluation of Cerium Doped Lutetium Oxyorthosilicate (LSO) Scintillation Crystal for PET. *IEEE Trans Nucl Sci* **40-4**: 1045-7 (1993).

[20] L.R. MacDonald, M. Dahlbom and M. Paulus. Investigation of Using PET Block Detector Technology for SPECT Imaging. *J. Nucl. Med.* **37**(5), May 1995.